Purdue University
Purdue e-Pubs

Other Nanotechnology Publications

Birck Nanotechnology Center

11-22-2006

Quantum Transport with Spin Dephasing: A Nonequilibrium Green's Function Approach

Ahmet Ali Yanik
Purdue University - Main Campus

Gerhard Klimeck
Purdue University - Main Campus, gekco@purdue.edu

Supriyo Datta
Purdue University - Main Campus

Follow this and additional works at: http://docs.lib.purdue.edu/nanodocs

Quantum Transport with Spin Dephasing:
A Nonequlibrium Green's Function Approach

Ahmet Ali Yanik*

Department of Physics, and
Network for Computational Nanotechnology,
Purdue University, West Lafayette, IN, 47907, USA

Gerhard Klimeck

School of Electrical and Computer Engineering,
Network for Computational Nanotechnology,
Purdue University, West Lafayette, IN, 47907, USA and
Jet Propulsion Lab, Caltech, Pasadena, CA, 91109, USA

Supriyo Datta

School of Electrical and Computer Engineering and
Network for Computational Nanotechnology,
Purdue University, West Lafayette, IN, 47907, USA

(Dated: November 22, 2006)

A quantum transport model incorporating spin scattering processes is presented using the non-equilibrium Green's function (NEGF) formalism within the self-consistent Born approximation. This model offers a unified approach by capturing the spin-flip scattering and the quantum effects simultaneously. A numerical implementation of the model is illustrated for magnetic tunnel junction devices with embedded magnetic impurity layers. The results are compared with experimental data, revealing the underlying physics of the coherent and incoherent transport regimes. It is shown that spin scattering processes are suppressed with increasing barrier heights while small variations in magnetic impurity spin-states/concentrations could cause large deviations in junction magnetoresistances.

PACS numbers: 72.10.-d, 72.25.-b, 72.25.Rb, 71.70.Gm, 73.43.Qt

I. INTRODUCTION

Quantum transport in spintronic devices is currently a topic of great interest. Most of the theoretical work reported so far has been based on the Landauer approach [1] assuming coherent transport, although a few authors have included incoherent processes through averaging over a large ensemble of disordered configurations [2–4]. However, it is not straightforward to include dissipative interactions in such approaches. The non-equilibrium Green's function (NEGF) formalism provides a natural framework for describing quantum transport in the presence of incoherent and dissipative processes. Here, a numerical implementation of the NEGF formalism with spin-flip scattering is presented. For magnetic tunnel junctions (MTJs) with embedded magnetic impurity layers, this model is able to capture and explain three distinctive experimental features reported in the literature [5–8] regarding the dependence of the junction magnetoresistances ($JMRs$) on (1) barrier thickness, (2) barrier height and (3) the number of magnetic impurities. The model is quite general and can be used to analyse and design a variety of spintronic devices beyond the 1-D

geometry explored in this article.

This article is organized as follows. In the view of pedagogical clarity, a heurisic presentation of the NEGF formalism with spin dephasing mechanisms is given Sec II followed by a numerical implementation of the model in Sec III. Initially (Sec III A) the definitions of device characteristics are presented for *impurity free* MTJs together with device parameters benchmarked against experimental measurements. How to incorporate the spin exchange scattering mechanisms into the electron transport calculations is shown (Sec III B), and the model is applied to MTJ devices with magnetic impurity layers (Sec III C). Theoretical estimates and experimental measurements are compared as well in this section (Sec III C), while a summary of the results is given in Sec IV.

II. MODEL DESCRIPTION

NEGF Method: The problem is partitioned into channel and contact regions as illustrated in Fig. 1 [9]. Components of the partitioned device can be classified in four categories:

(i) *Channel* properties are defined by the Hamiltonian matrix $[H]$ including the applied bias potential.

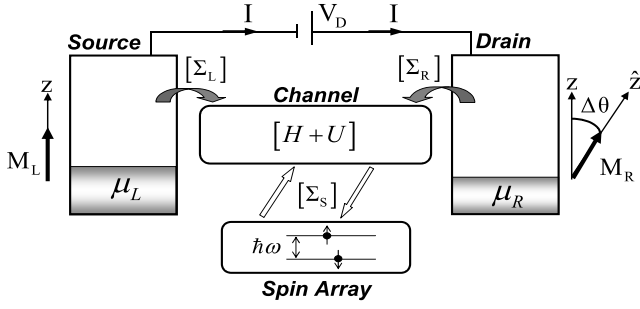(ii) *Contacts* are included through self-energy matrices

FIG. 1: Schematic illustration of the device partitioning with matrices needed for NEGF quantum transport calculations. Magnetization direction of the drain is defined relative to the source($\Delta\theta = \theta_R - \theta_L$).

$[\Sigma_L]/[\Sigma_R]$ whose anti-hermitian component:

$$\Gamma_{L,R}(E) = i\left(\Sigma_{L,R}(E) - \Sigma_{L,R}^+(E)\right), \qquad (1)$$

describes the broadening due to the coupling to the contact. The corresponding inscattering/outscattering matrices are defined as:

$$\Sigma_{L,R}^{in}(E) = f_0(E - \mu_{L,R})\Gamma_{L,R}(E), \qquad (2a)$$

$$\Sigma_{L,R}^{out}(E) = [1 - f_0(E - \mu_{L,R})]\Gamma_{L,R}(E), \qquad (2b)$$

where $f_0(E - \mu_{L,R}) = 1/1 + \exp[(E - \mu_{L,R})/k_BT]$ is the Fermi function for the related contact.

(iii) *Electron-electron interactions* are incorporated through the mean field electrostatic potential matrix $[U]$.

(iv) *Incoherent* scattering processes in the channel region are described by in/out-scattering matrices $[\Sigma_S^{in}]/[\Sigma_S^{out}]$. Broadening due to scattering is given by:

$$\Gamma_S(E) = \left[\Sigma_S^{in}(E) + \Sigma_S^{out}(E)\right], \qquad (3)$$

from which the self-energy matrix is obtained through a Hilbert transform:

$$\Sigma_S(E) = \overbrace{\frac{1}{2\pi}\int\frac{\Gamma_S(E')}{E' - E}dE'}^{\text{Re}} - i\overbrace{\frac{\Gamma_S(E)}{2}}^{\text{Im}}. \qquad (4)$$

Eqs. (1-A.13) are the boundary conditions that drive the coupled NEGF equations [Eqs. (3-8)], where Green's function is defined as:

$$G = [EI - H - U - \Sigma_L - \Sigma_R - \Sigma_S]^{-1}, \qquad (5)$$

with the spectral function (analogous to density states):

$$A = i[G - G^+] = G^n + G^p, \qquad (6)$$

where $[G^n]/[G^p]$ refer the *electron/hole correlation functions* (whose diagonal elements are the electron/hole density):

$$G^{n,p} = G\left[\Sigma_L^{in,out} + \Sigma_R^{in,out} + \Sigma_S^{in,out}\right]G^+. \qquad (7)$$

The in/out-scattering matrices $[\Sigma_S^{in}]/[\Sigma_S^{out}]$ are related to the electron/hole correlation functions $[G^n]/[G^p]$ through:

$$\Sigma_{S;\sigma_i\sigma_j}^{in,out}(r,r';E) = \int\sum_{\sigma_k,\sigma_l}\left[D_{\sigma_i\sigma_j;\sigma_k\sigma_l}^{n,p}(r,r';\hbar\omega)\right]_{sf}G_{\sigma_k\sigma_l}^{n,p}(r,r';E \mp \hbar\omega)\,d(\hbar\omega))$$
$$+ \int\sum_{\sigma_k,\sigma_l}\left[D_{\sigma_i\sigma_j;\sigma_k\sigma_l}^{n,p}(r,r';\hbar\omega)\right]_{nsf}G_{\sigma_k\sigma_l}^{n,p}(r,r';E)\,d(\hbar\omega). \qquad (8)$$

Here the spin indices (σ_k, σ_l) refer to the (2x2) block diagonal elements of the on-site electron/hole correlation function which is related through the $[D^n]/[D^p]$ tensors to the (σ_i, σ_j) spin components of the (2x2) block diagonal of the in/out-scattering function. This term can be interpreted as in the following. The first part describes the process of spin-flip transitions (subscript sf) due to the spin-exchange scatterings in the channel region. The second part denotes the contributions of the spin-conserving exchange scatterings (subscript nsf for "no spin-flip") in the channel region. Both of the contributing parts are previously shown by Appelbaum[10] using a similar treatment. Here the $[D^n]/[D^p]$ are fourth-order scattering tensors, describing the spatial correlation and the energy spectrum of the underlying microscopic *spin-dephasing* scattering mechanisms. These scattering tensors can be obtained from the spin scattering hamiltonian. In the Appendix, a second quantized operator based derivation is presented for $[D^n]/[D^p]$ tensors including the inelastic spin-flip transitions for an *isotropic* and *point like* electron-impurity spin exchange interaction of type:

$$H_{int}(\vec{r}) = \sum_{R_{jj}}J\left(\vec{r} - \vec{R}_{jj}\right)\vec{\sigma}\cdot\vec{S}_{jj}, \qquad (9)$$

where $\vec{r}/\vec{R}_{jj}$ are the spatial coordinates and $\vec{\sigma}/\vec{S}_{jj}$ are the spin operators for the *channel electron/(jj-th) magnetic-impurity*. For point like $\delta(r-r')$ and isotropic exchange scattering processes, the scattering tensor for the first

term in Eq. (8) corresponding to the spin-flip transitions can be given in matrix form with the proper indices relating the spin components:

$$
\begin{array}{c}
|\sigma_k \sigma_l\rangle \rightarrow \\
\langle \sigma_i \sigma_j| \downarrow
\end{array}
\quad
\begin{array}{cccc}
|\uparrow\uparrow\rangle & |\downarrow\downarrow\rangle & |\uparrow\downarrow\rangle & |\downarrow\uparrow\rangle
\end{array}
$$

$$
[\mathrm{D^{n,p}}(r,r';\hbar\omega)]_{\mathrm{sf}} = \sum_{\omega_q} J^2 N_I
\begin{array}{c}
\langle\uparrow\uparrow| \\
\langle\downarrow\downarrow| \\
\langle\uparrow\downarrow| \\
\langle\downarrow\uparrow|
\end{array}
\left[
\begin{array}{cccc}
0 & F_{u,d}\delta(\omega\pm\omega_q) & 0 & 0 \\
F_{d,u}\delta(\omega\pm\omega_q) & 0 & 0 & 0 \\
0 & 0 & 0 & 0 \\
0 & 0 & 0 & 0
\end{array}
\right]. \tag{10}
$$

Spin-flip transitions of electrons due to the exchange scattering processes can be *elastic/inelastic* depending on the degeneracy ($\hbar\omega = 0/\hbar\omega \neq 0$) of the impurity spin states. Whereas independetly from the energy difference between impurity spin states, spin-conserving exchange

scattering processes are *elastic* and their effect is mainly broadening of the electronic states. Accordingly, spin conserving scattering (no spin-flip) tensor in Eq. (8) is given as:

$$
\begin{array}{c}
|\sigma_k \sigma_l\rangle \rightarrow \\
\langle \sigma_i \sigma_j| \downarrow
\end{array}
\quad
\begin{array}{cccc}
|\uparrow\uparrow\rangle & |\downarrow\downarrow\rangle & |\uparrow\downarrow\rangle & |\downarrow\uparrow\rangle
\end{array}
$$

$$
[\mathrm{D^{n,p}}(r,r';\hbar\omega)]_{\mathrm{nsf}} = \sum_{\omega_q} \tfrac{1}{4}J^2 N_I[\delta(\omega-\omega_q)]
\begin{array}{c}
\langle\uparrow\uparrow| \\
\langle\downarrow\downarrow| \\
\langle\uparrow\downarrow| \\
\langle\downarrow\uparrow|
\end{array}
\left[
\begin{array}{cccc}
1 & 0 & 0 & 0 \\
0 & 1 & 0 & 0 \\
0 & 0 & -1 & 0 \\
0 & 0 & 0 & -1
\end{array}
\right]. \tag{11}
$$

Current is calculated from the self-consistent solution of the above equations for any terminal $"i"$:

$$
I_i = \frac{q}{h} \int\limits_{-\infty}^{\infty} trace\left(\left[\Sigma_i^{in}(E) A(E)\right] - \left[\Gamma_i(E) G^n(E)\right]\right) dE. \tag{12}
$$

A general solution scheme without going into the details can be summarized as follows . The matrices listed under the categories (i) and (ii) are fixed at the outset of any calculations. While the $[U]$, $[\Sigma_S^{in,out}]$ and $[\Sigma_S]$ matrices under the *charging and scattering* categories (iii) and (iv) depend on the correlation and spectral functions requiring an *iterative self-consisted solution* of the NEGF Equations [Eqs. (3-8)]. One important thing to note is that for the numerical implementation presented in Sec III we do not compute the charging potential $[U]$ self-consistently with the charge. The change in tunnel barriers is neglected and assumed not to influence the electrostatic potential. This allows one to focus on the *dephasing* due to the spin-flip interactions.

III. APPLICATION: MTJs WITH MAGNETIC IMPURITIES

Electron transport is considered *coherent* by standard definitions if through the course of electron's journey from source to drain state of nothing else changes. Accordingly scatterings from "rigid" impurities are considered as coherent processes whereas incoherent processes are mainly viewed as inelastic meaning they involve energy exchange between the electron and the impurities through which impurities are set into a jiggling motion. Yet it's not necessary that every incoherent process involves an exchange of energy between the electron and the impurity. A good example to this will be investigated in this part of the paper for electron-impurity spin exchange scattering processes in MTJs.

A. MTJs: Coherent Regime

In this section, MTJ device fundamentals and the tunneling transport characteristics are presented in the absence of magnetic impurities *(the coherent regime)*.
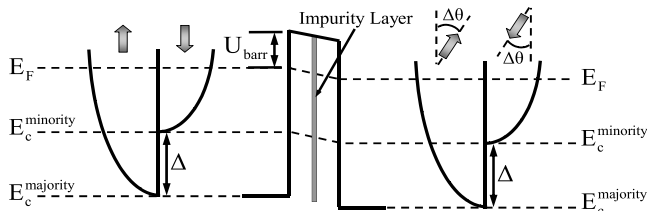
FIG. 2: Energy band diagram for the model MTJs.

MTJs devices considered here consist of a tunneling barrier (AlO$_x$) sandwiched between two ferromagnets (Co) with different magnetic coercivities enabling independent manipulation of contact magnetization directions (Fig. 2. Single band tight-binding approximation is adopted [11] with an effective electron mass ($m^* = m_e$) in the tunneling region and the ferromagnetic contacts.

$$E - H - \Sigma_L - \Sigma_R = \begin{array}{c} \langle 1| \\ \langle 2| \\ \vdots \\ \langle N-1| \\ \langle N| \end{array} \begin{bmatrix} EI - \alpha_1 - \Sigma_L & \beta & \cdots & \bar{0} & \bar{0} \\ \beta^+ & EI - \alpha_2 & \cdots & \bar{0} & \bar{0} \\ \vdots & \vdots & \ddots & \vdots & \vdots \\ \bar{0} & \bar{0} & \cdots & EI - \alpha_{N-1} & \beta \\ \bar{0} & \bar{0} & \cdots & \beta^+ & EI - \alpha_N - \Sigma_R \end{bmatrix}, \quad (14)$$

where α_n is a 2x2 on-site matrix:

$$\alpha_n = \begin{bmatrix} E_{c,n}^{\uparrow} + 2t + U_n & 0 \\ 0 & E_{c,n}^{\downarrow} + 2t + U_n \end{bmatrix}, \quad (15)$$

and $\beta_n = -tI$ is a 2x2 site-coupling matrix with $t = \hbar^2/2ma^2$ and $I = \left(\begin{smallmatrix} 1 & 0 \\ 0 & 1 \end{smallmatrix} \right)$. The left contact self-energy matrix is nonzero only for the first 2x2 block:

$$\Sigma_L (1,1; E_z) = \begin{bmatrix} -te^{ik_L^{\uparrow}a} & 0 \\ 0 & -te^{ik_L^{\downarrow}a} \end{bmatrix}, \quad (16)$$

where $E_z = E_c^{\uparrow,\downarrow} + U_L + 2t \left(1 - \cos k_L^{\uparrow,\downarrow}a \right)$. For the right contact only the last block is non-zero:

$$\Sigma_R (N,N,E_z) = \bar{U}^+ \begin{bmatrix} -te^{ik_R^{\uparrow}a} & 0 \\ 0 & -te^{ik_R^{\downarrow}a} \end{bmatrix} \bar{U}, \quad (17)$$

where $\bar{U}$ is the unitary transformation operator needed to obtain right contact self-energy matrix in the left contact magnetization spin basis set, if the polarization direction in two contacts differ by an angle $\Delta\theta$:

$$\tilde{U} (\Delta\theta) = \begin{bmatrix} \cos(\Delta\theta/2) & \sin(\Delta\theta/2) \\ -\sin(\Delta\theta/2) & \cos(\Delta\theta/2) \end{bmatrix}. \quad (18)$$

Accordingly for constant effective mass throughout the device, transverse modes can be included using 2-D integrated Fermi functions $f_{2D} (E_z - \mu_{L,R}) = \left(m^* k_B T / 2\pi\hbar^2 \right) \ln \left[1 + \exp \left(\mu_{L,R} - E_z / k_B T \right) \right]$ in Eq. (A.13) instead of numerically summing parallel k-components.

The Green's function of the device in the coherent regime is simply:

$$G = (E - H - \Sigma_L - \Sigma_R)^{-1}, \quad (13)$$

without any self-consistent solutions where H is Hamiltonian of the isolated system, and Σ_L/Σ_R are the self-energies due to the source/drain contacts. In real space for a discrete lattice whose points are located at $x = ja$, j being an integer ($j = 1 \cdots N$), the matrix $(E - H - \Sigma)$ can be expressed as:

A theoretical analysis of MTJ devices in the absence of magnetic impurity layers is presented and compared with the experimental data [5, 7] for varying tunneling barrier heights and thicknesses. The parameters used here for the generic ferromagnetic contacts are the Fermi energy $E_F = 2.2$ eV and the exchange field $\Delta = 1.45$ eV [11]. The tunneling region potential barrier [U_{barr}] is parameterized within the band gaps quoted from the literature [22, 23], while the charging potential [U] is neglected due to the pure tunneling nature of the transport.

Coherent tunneling regime features are obtained by benchmarking the experimental measurements made in impurity free tunneling oxide MTJs at small bias voltages. Referring to I_F/I_{AF} as the current values for the parallel/antiparallel magnetizations ($\Delta\theta = 0/\Delta\theta = \pi$) of the ferromagnetic contacts, the JMR is defined as:

$$JMR = (I_F - I_{AF})/I_F. \quad (19)$$

The dependence of the $JMRs$ on the thickness and the height of the tunneling barriers is shown in Fig. 3(a) with an energy resolved analysis [Fig. 3(b)] for different barrier thicknesses ($0.7 - 1.4 - 2.1$ nm). JMR values are shown to be improving with increasing barrier heights for all barrier thicknesses, a theoretically predicted [7, 8] and experimentally observed [12–21] feature in MTJs.
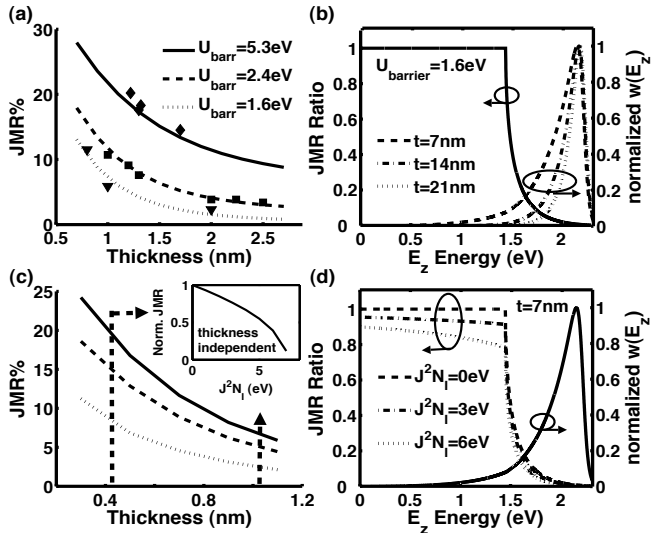
FIG. 3: For impurity free MTJs, (a)thickness dependence of $JMRs$ for different barrier heights are shown in comparison with experimental measurements [12–21] while an (b)energy resolved analysis of $JMR(E_z)$ *(left-axis)* and *normalized $w(E_z)$ (right-axis)* distributions is also presented for a device with a tunneling barrier height of *1.6 eV*. For MTJs with impurity layers, (c)variation of $JMRs$ for varying barrier thicknesses and interactions strengths are shown together with (d)an energy resolved analysis. Normalized $JMRs$ are proven to be thickness independent as displayed in the inset.

The barrier heights obtained here may differ from those reported in literature [12–21] based on empirical models [24].

Experiments and theoretical calculations observe deterioration of $JMRs$ with increasing barrier thicknesses [Fig. 3(a)]. Whereas an energy resolved theoretical analysis shows that energy by energy junction magnetoresistances defined as:

$$JMR(E_z) = (I_F(E_z) - I_{AF}(E_z))/I_F(E_z), \qquad (20)$$

remain unchanged [Fig. 3(b)]. This initially counter intuitive observation can be understood by considering the redistribution of tunneling electron densities over energies with changing tunneling barrier thicknesses. Defining $w(E_z)$ as a measure of the contributing weight of the $JMR(E_z)$, one can show that experimentally measured JMR is a weighted integral of $JMR(E_z)$s over energies E_z:

$$JMR = \int \omega(E_z) JMR(E_z) dE_z, \qquad (21)$$

where $\omega(E_z) = I_F(E_z)/I_F$ is the energy resolved *spin-continuum current component* (weighting function). In Eq. (21), independently from the barrier thicknesses

$JMR(E_z)$ ratios are *constant* (solid line in Fig. 3(b)), while the *normalized $w(E_z)$* distributions shifts towards higher energies with increasing barrier thicknesses (dashed lines in Fig. 3(b)). Hence $JMRs$, an integral of the multiplication of the $w(E_z)$ distributions with the energy resolved $JMR(E_z)$s, deteriorates with increasing barrier thicknesses (Eq. (19)).

B. Adding Spin Exchange Scattering

Spin exchange scattering processes are responsible from the incoherent nature of the tunneling transport for the model devices considered here. Through this elastic scattering process, the state of nothing else seem to change if the electron and the impurity spins are considered as a composite system. Nevertheless, it is an incoherent process since the state of the impurity has changed. What makes this process incoherent are the external forces forcing the impurity spins into local equilibrium. The incoherent nature of the scattering lies in the "information erasure" of the surrounding through the forces forcing the impurity spins into an unpolarized (%50 up, %50 down) spin distribution. These external forces in a closely packed impurity layer can be magnetic dipole-dipole interactions among the magnetic impurities or spin relaxation processes coupled with phononic excitations. Nevertheless the physical origin of the equilibrium restoring processes is not of our interest (at least from tunneling electron's point of view) assuming equilibrium restoring processes are fast enough to maintain the impurity spins in a thermal equilibrium state. Accordingly, NEGF formalism incorporates spin dephasing effects of the environment into the electron transport problem through a boundary condition (the spin-scattering self-energy). As discussed in Sec II, coupling between the number of available electrons/holes ($[G^n]/[G^p]$) at a state and the in/out-flow ($[\Sigma_S^{in}]/[\Sigma_S^{out}]$) to/from that state is related through the fourth order scattering tensor $[D^n]/[D^p]$ in Eq. (8).

For the model systems considered here magnetic impurity spin states are degenerate ($\hbar\omega = 0$) allowing only elastic spin-flip transitions. Spin-conserving scattering processes are also neglected due to their minor effect on the JMRs. Accordingly, for isotropic and point like ($\delta(r - r')$) spin exchange scattering tensor relationship given in Eq. (8) will simplify to:

$$\Sigma_S^{in,out}(r,r;E) = \left[D_{\sigma_i\sigma_j;\sigma_k\sigma_l}^{n,p}\right]_{sf} G_{\sigma_k\sigma_l}^{n,p}(r,r;E). \qquad (22)$$

$[D^n]/[D^p]$ scattering tensors relate the electron/hole $[G^n]/[G^p]$ correlation matrices with the (2x2) block diagonal elements of $[\Sigma_S^{in}]/[\Sigma_S^{out}]$ in/out-scattering matrices of form:

$$
\Sigma_S^{in,out} = \begin{pmatrix} \left(\bar{\Sigma}_S^{in,out}\right)_{1,1} & \bar{0} & \cdots & \bar{0} \\ \bar{0} & \left(\bar{\Sigma}_S^{in,out}\right)_{2,2} & \cdots & \bar{0} \\ \vdots & \vdots & \ddots & \vdots \\ \bar{0} & \bar{0} & \cdots & \left(\bar{\Sigma}_S^{in,out}\right)_{N,N} \end{pmatrix}, \tag{23}
$$

through the tensor relationship *(shown below in matrix format)* for the corresponding lattice site "j" with magnetic impurities:

$$
\begin{bmatrix} \left(\Sigma_{S;\uparrow\uparrow}^{in,out}\right)_{jj} \\ \left(\Sigma_{S;\downarrow\downarrow}^{in,out}\right)_{jj} \\ \left(\Sigma_{S;\uparrow\downarrow}^{in,out}\right)_{jj} \\ \left(\Sigma_{S;\downarrow\uparrow}^{in,out}\right)_{jj} \end{bmatrix} = J^2 N_I \overbrace{\begin{bmatrix} 0 & F_{u,d} & 0 & 0 \\ F_{d,u} & 0 & 0 & 0 \\ 0 & 0 & 0 & 0 \\ 0 & 0 & 0 & 0 \end{bmatrix}}^{[D^{n,p}]_{sf}} \begin{bmatrix} \left(G_{\uparrow\uparrow}^{n,p}\right)_{jj} \\ \left(G_{\downarrow\downarrow}^{n,p}\right)_{jj} \\ \left(G_{\uparrow\downarrow}^{n,p}\right)_{jj} \\ \left(G_{\downarrow\uparrow}^{n,p}\right)_{jj} \end{bmatrix},
\tag{24}
$$

where N_I is the number of magnetic impurities and F_u/F_d represents fractions of spin-up/spin-down impurities for an uncorrelated ensemble ($F_u + F_d = 1$).

This tensor relationship can be understood heuristically from elementary arguments. The in/out-scattering into *spin-up* component is proportional to the density of the *spin-down electrons/holes* times the number of *spin-up impurities*, $N_I F_u$:

$$
\left(\Sigma_{S,\uparrow\uparrow}^{in,out}\right)_{jj} = J^2 N_I F_u \left(G_{\downarrow\downarrow}^{n,p}\right)_{jj}. \tag{25}
$$

Similarly, the in/out-scattering into *spin-down* component is proportional to the density of the *spin-up electrons/holes* times the number of *spin-down impurities*, $N_I F_d$:

$$
\left(\Sigma_{S,\downarrow\downarrow}^{in,out}\right)_{jj} = J^2 N_I F_d \left(G_{\uparrow\uparrow}^{n,p}\right)_{jj}. \tag{26}
$$

C. Incoherent Regime: Results

The *incoherent* tunneling regime device characteristics in the presence of magnetic impurities is studied for a fixed barrier height $U_{barr} = 1.6$ eV [Fig. 3 (c)] with changing barrier thicknesses and electron-impurity spin exchange interactions ($J^2 N_I = 0 - 6$ eV). A *nonlinear* deterioration of $JMRs$ with increasing spin-exchange interactions is observed at all barrier thicknesses due to the mixing of independent spin-channels [5, 6] while the *normalized JMRs* are proven to be thickness independent *(inset)*. This observation is attributed to the elastic nature of the spin exchange interactions yielding a total drop in $JMR(E_z)$ values at all E_z energies in Eq. (19)

while preserving the *normalized* $\omega(E_z)$ carrier distributions [Fig. 3(d)].

Further analysis shows that *"normalized" JMRs* of the MTJs with magnetic impurity layers converges to that of the impurity free ($J^2 N_I = 0$) MTJs with increasing barrier heights [Fig. 4(a)]. This observation demonstrates that the spin channel mixing of the exchange scattering processes are suppressed with increasing barrier heights. This is in agreement with previous predictions for impurity free MTJs [7, 7]. Another interesting feature is that *"normalized" JMRs* deteriorates with increasing spin-dephasing strengths ($J^2 N_I$) independently from the tunneling barrier heights [Fig. 4(b)]. This general trend can be shown by mapping the *"normalized" JMRs* into a *single universal curve* using a tunneling barrier height dependent scaling constant $c(U_{barr})$ (inset in Fig. 4(b)).
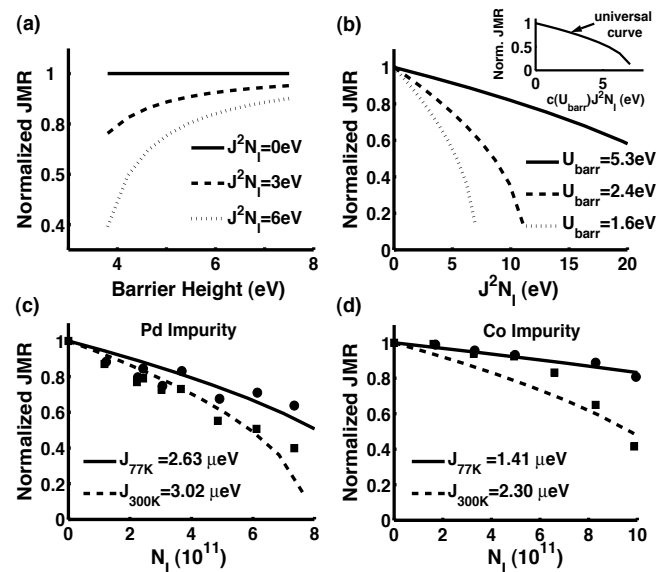

FIG. 4: (a) *"Normalized" JMRs* of the MTJs with magnetic impurities converges to that of the impurity free ($J^2 N_I = 0$) MTJs with increasing barrier heights. (b) *Normalized JMRs* deteriorates with increasing spin-dephasing strengths independently from the tunneling barrier heights. This general trend can be scaled to a *single universal curve* (inset). Experimental data taken at $77K$ and $300K$ is compared with theoretical analysis in the presence of (c) palladium and (d) cobalt magnetic impurities with increasing impurity concentrations.

This allows us to choose a particular value of barrier height [$U_{barr} = 1.6eV$] and adjust a *single parameter* J to fit our NEGF calculations [Fig. 4(c-d)] with experimental measurements obtained from δ-doped MTJs [5]. Submonolayer impurity thicknesses given in the measurements are converted into number of impurities using material concentrations of Pd/Co impurities and device cross sections (6×10^{-4} cm^2) [5].

Close fitting to the experimental data are observed at $77K$ [Fig. 4(c-d)] using physically reasonable exchange coupling constants of $J = 2.63\mu eV/1.41\mu eV$ for devices with Pd/Co impurities [25]. However, experimentally observed temperature dependence of *normalized JMR* ratios can not be accounted for by our model calculations. Broadenings of the electrode Fermi distributions due to changing temperatures from $77K$ to $300K$ seem to yield variations in *normalized JMR* ratios within a linewidth. As a result, different J exchange couplings are used in order to match the experimental data taken at 300K.

For *Pd doped* MTJs, a relatively small variation in J exchange couplings is needed ($J_{300}/J_{77} = 1.16$) in order to match the experimental data at 300K. This small temperature dependence could be due to the presence of some secondary mechanisms not included in our calculations. One such mechanism reported in literature includes the presence of impurity-assisted conductance contribution through the defects *(possibly created by the inclusion of magnetic impurities within the barrier)* which is known to be strongly temperature dependent [26]. In fact, the contribution of the impurity-assistant conductance is proportional with the impurity concentrations in accordance with the experimental measurements [Fig. 4(c)].

On the contrary, for *Co doped* MTJs, there's a clear distinction for *normalized JMR* ratios at different temperatures [Fig. 4(d)] which can not be justified by the presence of secondary mechanisms. Fitting these large deviations require large variations in J exchange coupling parameters [$J_{300}/J_{77} = 1.73$] We propose this to be a result of thermally driven *low-spin/high-spin phase* transition [27, 28], since the oxidation state of the cobalt atoms can be in Co^{+2} ($S = 3/2$, high-spin) or Co^{+3} ($S = 0$, low-spin) state or partially in both of the states depending on the oxidation environment. Such thermally driven low-spin/high-spin phase transitions for metal-oxides has been predicted by theoretical calculations and observed in previous experimental studies [27, 28]. These phase transitions have not been discussed in MTJs community in connection with possible scattering factors determining the temperature dependence of *JMRs*. Although from the avaliable experimental data it's not possible to make a decisive conclusion in this direction, given the non-linear dependence of *JMRs* on magnetic impurity states in our calculations, we believe it's important to point out this possibility here.

IV. SUMMARY

Summary: A NEGF based quantum transport model incorporating spin-flip scattering processes within the self-consistent Born approximation is presented. Spin-flip scattering and quantum effects are simultaneously captured. Spin scattering operators are derived for the specific case of electron-impurity spin-exchange interactions and the formalism is applied to spin dependent electron transport in MTJs with magnetic impurity layers. The theory is benchmarked against experimental data involving both coherent and incoherent transport regimes. *JMRs* are shown to decrease both with barrier thickness and with spin-flip scattering but our unified treatment clearly brings out the difference in the underlying physics [Fig. 3]. The deteriorating effect of the magnetic impurities on *JMR* ratios diminishes with increasing tunneling barrier heights [Fig. 4(a)]. Our numerical results show that both barrier height and the exchange interaction constant J can be subsumed into a single parameter that can explain a variety of experiments [Fig. 4]. Interesting differences between devices having Pd and Co impurities are pointed out, which could be signatures of low-spin/high-spin phase transitions in cobalt oxides. Small differences in spin-states/concentrations of magnetic impurities are shown to cause large deviations in *JMRs*.

Acknowledgments

APPENDIX: SPIN DEPHASING SELF ENERGY

In the following, scattering tensors are derived for point like electron-impurity spin exchange interactions by using a second quantized operator treatment involving both electron and impurity spin states. This approach should give correct results at least to the first order, so-called self-consistent Born approximation. This self-energy matrix treatment has been successfully applied for the electron-phonon and electron-electron scattering processes in literature [9, 29] although according to our knowledge it has not been applied to spin dephasing processes except through a heuristic approach for elastic ($\hbar\omega = 0$) impurity scattering processes by Datta [30]. Here self energy treatment is extended to incorporate inelastic spin scattering processes ($\hbar\omega \neq 0$) as well following previous second quantized operator treatments [9, 31, 32]. A typo for the exchange scattering tensor given in Eq. (A.9b) in [30] is also corrected here.

The in/out-scattering function representing the correlation of the source terms can be expressed as [9]:

$$\Sigma_{ij}^{in}(r, r'; t, t') \equiv \left\langle S_j^+(r', t') S_i(r, t) \right\rangle. \qquad \text{(A.1a)}$$

$$\Sigma_{ij}^{out}(r, r'; t, t') \equiv \left\langle S_i(r, t) S_j^+(r', t') \right\rangle. \qquad \text{(A.1b)}$$

Here the subscripts correspond to spin states in electron subspace. Through Jordan-Wigner transformation, single spins can be thought as an empty or singly occupied fermion state:

$$|\uparrow\rangle \equiv a^+ |0\rangle, \qquad \text{(A.2a)}$$

$$|\downarrow\rangle \equiv |0\rangle, \qquad \text{(A.2b)}$$

where the *creation/annihilation* operators are:

$$a^+ = \sigma^+ = \begin{bmatrix} 0 & e^{i\omega_e t} \\ 0 & 0 \end{bmatrix}, \qquad \text{(A.3a)}$$

$$a = \sigma^- = \begin{bmatrix} 0 & 0 \\ e^{-i\omega_e t} & 0 \end{bmatrix}. \qquad \text{(A.3b)}$$

Accordingly, source terms are defined as:

$$S_i(r, t) = \sum_k \tau_{ik}(r, t) a_k(t), \qquad \text{(A.4a)}$$

$$S_j^+(r', t') = \sum_l \tau_{jl}^*(r', t') a_l^+(t')$$
$$= \sum_l \tau_{lj}^+(r', t') a_l^+(t'), \qquad \text{(A.4b)}$$

where for a given spin scattering exchange interaction Hamiltonian H_{int}:

$$\tau_{ik}(r, t) = \langle i| H_{\text{int}}(r, t) |j\rangle, \qquad \text{(A.5a)}$$

$$\tau_{jl}(r', t') = \langle i| H_{\text{int}}^+(r', t') |j\rangle. \qquad \text{(A.5b)}$$

For point like ($\delta(r - r')$) scattering processes, substituting source term Eq. (A.4) into Eq. (A.1) will yield:

$$\Sigma_{ij}^{in}(t, t') = \left\langle \sum_k \tau_{ik}(t) \left[a_l^+(t') a_k(t') \right] \sum_l \tau_{lj}^+(t') \right\rangle. \qquad \text{(A.6)}$$

Fourier transform of this relation will simplify further if the electron spin states are degenerate ($\hbar\omega_e = 0$):

$$\Sigma_{ij}^{in}(E) = \left\langle \sum_k \tau_{ik}(t) \sum_l \tau_{lj}^+(t') \right\rangle_{FT} G_{kl}^n(E), \qquad \text{(A.7)}$$

where $G_{ik}^n(E) = \left\langle a_k^+(t') a_i(t) \right\rangle_{FT}$. Accordingly $[D^n(E)]$ and $[D^p]$ are given as:

$$D_{ij;kl}^n(\hbar\omega) = \left\langle \sum_k \tau_{ik}(t) \sum_l \tau_{lj}^+(t') \right\rangle_{FT}$$
$$= \left\langle \langle i| H_{\text{int}}(t) |k\rangle \langle l| H_{\text{int}}^+(t') |j\rangle \right\rangle_{FT}, \qquad \text{(A.8a)}$$

$$D_{ij;kl}^p(\hbar\omega) = \left\langle \sum_k \tau_{ik}^+(t) \sum_l \tau_{lj}(t') \right\rangle_{FT}$$
$$= \left\langle \langle i| H_{\text{int}}^+(t) |k\rangle \langle l| H_{\text{int}}(t') |j\rangle \right\rangle_{FT}, \qquad \text{(A.8b)}$$

where exchange scattering Hamiltonian [Eq. (9)] is expressed in terms of second quantized operators as:

$$H_{\text{int}}(r, t) = J\delta\left(\vec{r} - \vec{R}\right) \left[\frac{1}{2} a S_+(t) + \frac{1}{2} a^+ S_-(t) + \left(a^+ a - \frac{1}{2} \right) S_z(t) \right]. \qquad \text{(A.9)}$$

Substituting the interaction Hamiltonian from Eq. (A.9) into Eq. (A.10) will yield:

$$
\begin{array}{c}
|\sigma_k \sigma_l\rangle \rightarrow \\
\langle\sigma_i\sigma_j|\downarrow
\end{array}
\quad
\begin{array}{cccc}
|\uparrow\uparrow\rangle & |\downarrow\downarrow\rangle & |\uparrow\downarrow\rangle & |\downarrow\uparrow\rangle
\end{array}
$$

$$
D^n(\hbar\omega)/J^2 =
\begin{array}{c}
\langle\uparrow\uparrow| \\
\langle\downarrow\downarrow| \\
\langle\uparrow\downarrow| \\
\langle\downarrow\uparrow|
\end{array}
\left[
\begin{array}{cccc}
\langle S_z(t) S_z(t')\rangle & \langle S_+(t) S_-(t')\rangle & \langle S_+(t) S_z(t')\rangle & \langle S_z(t) S_-(t')\rangle \\
\langle S_-(t) S_+(t')\rangle & \langle S_z(t) S_z(t')\rangle & -\langle S_z(t) S_+(t')\rangle & -\langle S_-(t) S_z(t')\rangle \\
\langle S_-(t) S_z(t')\rangle & -\langle S_z(t) S_-(t')\rangle & -\langle S_z(t) S_z(t')\rangle & \langle S_-(t) S_-(t')\rangle \\
\langle S_z(t) S_+(t')\rangle & -\langle S_+(t) S_z(t')\rangle & \langle S_+(t) S_+(t')\rangle & -\langle S_z(t) S_z(t')\rangle
\end{array}
\right]_{FT} , \quad (A.10a)
$$

$$
\begin{array}{c}
|\sigma_k \sigma_l\rangle \rightarrow \\
\langle\sigma_i\sigma_j|\downarrow
\end{array}
\quad
\begin{array}{cccc}
|\uparrow\uparrow\rangle & |\downarrow\downarrow\rangle & |\uparrow\downarrow\rangle & |\downarrow\uparrow\rangle
\end{array}
$$

$$
D^p(\hbar\omega)/J^2 =
\begin{array}{c}
\langle\uparrow\uparrow| \\
\langle\downarrow\downarrow| \\
\langle\uparrow\downarrow| \\
\langle\downarrow\uparrow|
\end{array}
\left[
\begin{array}{cccc}
\langle S_z(t) S_z(t')\rangle & \langle S_-(t) S_+(t')\rangle & \langle S_z(t) S_+(t')\rangle & \langle S_-(t) S_z(t')\rangle \\
\langle S_+(t) S_-(t')\rangle & \langle S_z(t) S_z(t')\rangle & -\langle S_+(t) S_z(t')\rangle & -\langle S_z(t) S_-(t')\rangle \\
\langle S_z(t) S_-(t')\rangle & -\langle S_-(t) S_z(t')\rangle & -\langle S_z(t) S_z(t')\rangle & \langle S_-(t) S_-(t')\rangle \\
\langle S_+(t) S_z(t')\rangle & -\langle S_z(t) S_+(t')\rangle & \langle S_+(t) S_+(t')\rangle & -\langle S_z(t) S_z(t')\rangle
\end{array}
\right]_{FT} , \quad (A.10b)
$$

where the spin-operators are defined in the *impurity spin-subspace* as:

$$
S^+ = d^+ = \begin{bmatrix} 0 & e^{i\omega t/\hbar} \\ 0 & 0 \end{bmatrix}, \quad (A.11a)
$$

$$
S^- = d = \begin{bmatrix} 0 & 0 \\ e^{-i\omega t/\hbar} & 0 \end{bmatrix}, \quad (A.11b)
$$

$$
S_z = d^+ d - \frac{1}{2} = \frac{1}{2}\begin{bmatrix} 1 & 0 \\ 0 & -1 \end{bmatrix}. \quad (A.11c)
$$

Operator expectation values can be obtained by $\langle A\rangle = trace(\rho A)$. For a given impurity density matrix of the form (Fu+Fd=1):

$$
\rho = N_I \begin{bmatrix} F_u & 0 \\ 0 & F_d \end{bmatrix}, \quad (A.12)
$$

where N_I being total number of impurities, the desired quantities $[D^n]/[D^p]$ are obtained by evaluating the expectation values of the operators in Eqs. (A.10a) and (A.10b): Only non-zero elements are obtained as:

$$
\langle S_z(t) S_z(t')\rangle = \frac{1}{4}, \quad (A.13a)
$$

$$
\langle S_+(t) S_-(t')\rangle = F_u e^{i\omega(t-t')}, \quad (A.13b)
$$

$$
\langle S_-(t) S_+(t')\rangle = F_d e^{i\omega(t'-t)}. \quad (A.13c)
$$

Finally, for a given impurity density matrix [Eq (A.12)], $[D^n]/[D^p]$ tensors are obtained as:

$$
\begin{array}{c}
|\sigma_k \sigma_l\rangle \rightarrow \\
\langle\sigma_i\sigma_j|\downarrow
\end{array}
\quad
\begin{array}{cccc}
|\uparrow\uparrow\rangle & |\downarrow\downarrow\rangle & |\uparrow\downarrow\rangle & |\downarrow\uparrow\rangle
\end{array}
$$

$$
D^n(t,t') = \sum_q J^2 N_I
\begin{array}{c}
\langle\uparrow\uparrow| \\
\langle\downarrow\downarrow| \\
\langle\uparrow\downarrow| \\
\langle\downarrow\uparrow|
\end{array}
\left[
\begin{array}{cccc}
1/4 & F_u e^{i\omega(t-t')} & 0 & 0 \\
F_d e^{i\omega(t'-t)} & 1/4 & 0 & 0 \\
0 & 0 & -1/4 & 0 \\
0 & 0 & 0 & -1/4
\end{array}
\right] , \quad (A.14a)
$$

$$
\begin{array}{c}
|\sigma_k \sigma_l\rangle \rightarrow \\
\langle\sigma_i\sigma_j|\downarrow
\end{array}
\quad
\begin{array}{cccc}
|\uparrow\uparrow\rangle & |\downarrow\downarrow\rangle & |\uparrow\downarrow\rangle & |\downarrow\uparrow\rangle
\end{array}
$$

$$
D^p(t,t') = \sum_q J^2 N_I
\begin{array}{c}
\langle\uparrow\uparrow| \\
\langle\downarrow\downarrow| \\
\langle\uparrow\downarrow| \\
\langle\downarrow\uparrow|
\end{array}
\left[
\begin{array}{cccc}
1/4 & F_d e^{i\omega(t'-t)} & 0 & 0 \\
F_u e^{i\omega(t-t')} & 1/4 & 0 & 0 \\
0 & 0 & -1/4 & 0 \\
0 & 0 & 0 & -1/4
\end{array}
\right] , \quad (A.14b)
$$

Once the fourier transforms are taken this equation will simplify to Eq (??) and Eq (11). For the calcula-

tions done in the article, diagonal elements not leading to spin-dephasing are omitted due to their negligible effect on JMR ratios. In this case $[D^n]/[D^p]$ scattering tensors simplifies to a form (Eq. (24)) which can be understood from simple common-sense arguments (Eqs. (25) and (26)).

[1] R. Landauer, Physica Scripta **T42**, 110 (1992).
[2] Y. Li and C. Chang, Phys. Lett. A **287**, 415 (2001).
[3] C. C. Y.Li and Y. Yao, J. Appl. Phys. **91**, 8807 (2002).
[4] D. X. L. Sheng and D. N. Sheng, Phys. Rev. B **69**, 132414 (2004).
[5] R. Jansen and J. Moodera, J. of Appl. Phys. **83**, 6682 (1998).
[6] R. Jansen and J. Moodera, Phys. Rev. B. **61**, 9047 (1998).
[7] A. Davis, Ph.D. thesis, Tulane University (1994).
[8] J. M. A.H. Davis, J. Phys.: Condens. Matter **14**, 4365 (2002).
[9] S. Datta, *Quantum Transport: Atom to Transistor* (Cambridge University Press, Cambridge, 2005).
[10] J. Appelbaum, Phys. Rev. **154**, 633 (1967).
[11] M. Stearns, J. Magn. Magn. Mater. **5**, 167 (1977).
[12] T. M. K. Matsuda, A. Kamijo and H. Tsuge, J. of Appl. Phys. **85**, 5261 (1999).
[13] G. N. J. L. H. S. S. Y. Z. H. Chen, Q. Y. Xu and Y. W. Du, J. of Appl. Phys. **85**, 5798 (1999).
[14] J. Zhang and R. M. White, J. of Appl. Phys. **83**, 6512 (1998).
[15] A. K. T. Mitsuzuka, K. Matsuda and H. Tsuge, J. of Appl. Phys. **85**, 5807 (1998).
[16] R. C. W. Oepts, H. J. Verhagen and W. J. M. de Jonge, J. of Appl. Phys. **86**, 3863 (1999).
[17] J. D. B. A. E. R. S. Beech, J. Anderson and D. Wang, IEEE Trans. Mag. **32**, 4713 (1996).
[18] K. T. H. F. H. Yamanaka, K. Saito, IEEE Trans. Mag. **35**, 2883 (1999).
[19] J. N. J.S. Moodera and R. van de Veerdonk, Phys. Rev. Lett. **80**, 2941 (1998).
[20] J. Sun and P. Freitas, J. of Appl. Phys. **85**, 5264 (1999).
[21] R. J. C.H. Shang, J. Nowak and J. Moodera, Phys. Rev. B **58**, 2917 (1998).
[22] J. Moodera and L. Kinder, Phys. Rev. Lett. **74**, 3273 (1995).
[23] V. Henrich and P. Cox, *The Surface Science of Metal Oxides* (Cambridge University Press, Cambridge, 1994).
[24] J. Simmons, J. Appl. Phys. **34**, 1793 (1963).
[25] B. Kane, Nature **393**, 133 (1998).
[26] R. S. et al., J. of Appl. Phys. **85**, 5258 (1999).
[27] T. Kambara, J. Chem. Phys. **70**, 4199 (1979).
[28] S. Biernacki and B. Clerjaud, Phys. Rev. B. **72**, 024406 (2005).
[29] R. C. B. R. Lake, G. Klimeck and D. Jovanovic, J. of Appl. Phys. **81** (1997).
[30] S. Datta, Proc. of Inter. School of Phys. Societa Italiana di Fisica p. 244 (2004).
[31] G. Mahan, Phys. Rep. **145**, 251 (1987).
[32] J. Rammer and H. Smith, Rev. Mod. Phys. **58** (1986).